Asymmetric Growth of Bilayer Graphene on Copper Enclosures Using Low-Pressure Chemical Vapor Deposition

Wenjing Fang,[†,⊥] Allen L. Hsu,[†,⊥] Yi Song,[†] Anthony G. Birdwell,[§] Matin Amani,[§] Madan Dubey,[§] Mildred S. Dresselhaus,[†,‡] Tomás Palacios,[†] and Jing Kong[†,*]

[†]Department of Electrical Engineering and Computer Sciences and [‡]Department of Physics, Massachusetts Institute of Technology, 77 Mass Avenue, Cambridge, Massachusetts 02139, United States, and [§]U.S. Army Research Laboratory, 2800 Powder Mill Road, Adelphi, Maryland 20783, United States. [⊥]These authors contributed equally to this work.

ABSTRACT In this work, we investigated the growth mechanisms of bilayer graphene on the outside surface of Cu enclosures at low pressures. We observed that the asymmetric growth environment of a Cu enclosure can yield a much higher (up to 100%) bilayer coverage on the outside surface as compared to the bilayer growth on a flat Cu foil, where both sides are exposed to the same growth environment. By simultaneously examining the graphene films grown on both the outside and inside surfaces of the Cu enclosure, we find that carbon can diffuse from the inside surface to the outside *via* exposed copper regions on the inside surface. The kinetics of this process are examined by coupling the asymmetric growth between the two surfaces through a carbon diffusion model. Finally, using these results, we show that the coverage of bilayer graphene can be tuned simply by changing the thickness of the Cu foil, further confirming our model of carbon delivery through the Cu foil.

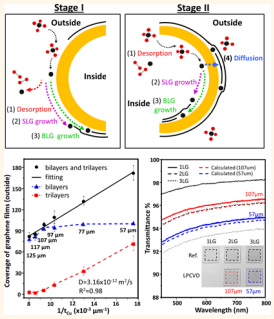

KEYWORDS: bilayer graphene · Cu enclosure · growth mechanism · carbon diffusion

Bilayer graphene has attracted considerable attention due to its unique electrical properties.[1,2] For instance, AB-stacked bilayer graphene exhibits a tunable band gap with an applied external electrical field,[3] which is promising for graphene-based electronic and photonic applications.[4−6] However, bilayer graphene flakes prepared by mechanical exfoliation are limited in size (∼5−15μm), and the process provides little control over their thickness or shape. In recent years, chemical vapor deposition (CVD) has emerged as a scalable method for producing large-area graphene films of varying thickness.[7−9] The synthesis of single- to few-layer graphene films has earlier been demonstrated using transition metals as substrates.[7−14] To date, copper substrates are more commonly used than nickel for monolayer growth because of copper's lower carbon solubility and dominant surface-limited growth. However, these properties also make it quite challenging to grow bilayers on copper; the catalytic copper surface becomes passivated by the monolayer graphene.[15] Nevertheless, several groups have reported methods of synthesizing bilayer graphene *via* CVD by controlling the carbon solubility of the catalyst, for example, using Cu−Ni alloy foils or Cu−Ni thin films.[16,17] However, bilayer graphene grown by increasing the carbon solubility of the substrate relies on a careful control of the alloy composition and the precipitation rate. Another approach to growing bilayers on copper involves introducing external carbon sources to deposit an additional layer on top of an existing monolayer.[18,19] In addition, direct growth of large domains of bilayer graphene from underneath discontinuous monolayer domains has also been reported, but with relatively low bilayer coverage.[20]

For a typical graphene growth under low-pressure CVD (LPCVD) using flat Cu foils, the growth of bilayer stops when the Cu surface is fully covered by graphene.[9,21,22] In our previous investigation, we have found that the limited coverage of bilayer graphene can be overcome by utilizing a Cu enclosure geometry.[21] In this work, we examined the coupling of the graphene growth between both inside and outside surfaces and investigated the passage ways of carbon.

* Address correspondence to jingkong@mit.edu.

Received for review September 14, 2013 and accepted May 30, 2014.

Published online May 30, 2014
10.1021/nn5015177

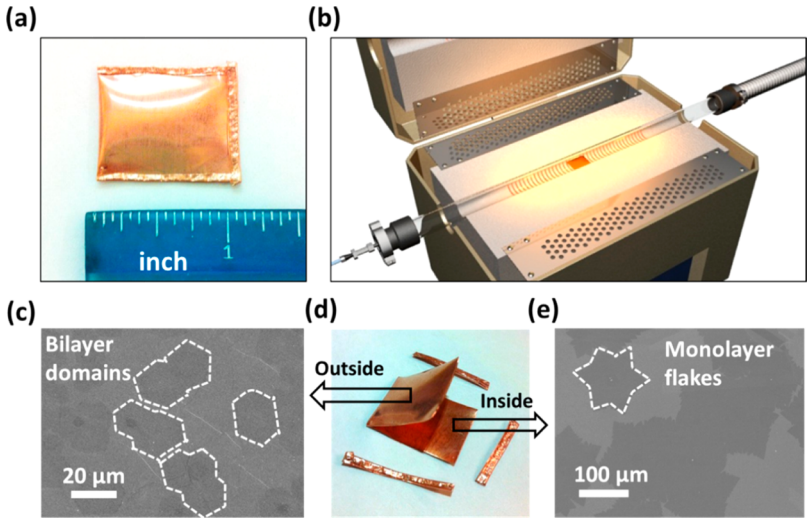

Figure 1. Cu enclosure and graphene grown on the Cu enclosures. (a) Photograph of a Cu enclosure. (b) Illustration of the CVD system with the Cu enclosure in the center of the heating zone. (c) SEM image of the outside surface of a Cu enclosure, where some of the hexagonal bilayer graphene domains are outlined by the white dotted line. (d) Photograph of an open Cu enclosure after growth. (e) SEM image of the dendritic monolayer graphene flakes on the inside surface of a Cu enclosure, where an isolated dendrite is outlined by the white dotted line.

We found that the diffusion of active carbon species (atomic carbon radicals and/or CH_x) through the Cu foil from the inside surface to the outside surface can circumvent the saturation of the bilayer graphene domain size, which can be observed on flat Cu foils. For example, after the completion of the monolayer growth on the outside, bilayers continue to grow on the outside by the carbon introduced from the exposed copper on the inside. The kinetics of the bilayer graphene on the outside are modeled assuming a carbon diffusion-limited model, which agrees well with the available experimental data. Finally, high-coverage bilayer films are achieved by tuning the rate of carbon delivery through the Cu foil.

RESULTS AND DISCUSSION

Graphene Growth on Cu Enclosure. The Cu enclosure method was previously initiated by Li *et al.* for the synthesis of large single-crystalline domain graphene flakes.[23] It has also been found that this geometry also favors the growth of bilayer graphene.[21] Figure 1a shows the Cu enclosure, and Figure 1b shows the CVD system used in this experiment. After growing for 1 h at 1050 °C under 1.5 sccm CH_4 and 50 sccm H_2, the Cu enclosure was opened (Figure 1d), and graphene domains could be observed on both the outside and inside surfaces by scanning electron microscopy (SEM), as shown in Figure 1c,e, respectively. Hexagonal bilayer domains of approximately 20 μm were observed on the outside surface, while large-area (up to hundreds of micrometers) dendritic monolayer flakes were found on the inside surface, consistent with previous reports.[21,23] Although a study of the bilayer growth on the inside surface has been performed in previous studies, we have focused on the outside surface due to the higher bilayer graphene coverage that was observed.[23]

Here we investigate the growth mechanism by comparing the graphene films grown on both sides of the Cu enclosure for different lengths of time, as shown in Figure 2. All the graphene layers were grown at 1050 °C under 1.5 sccm CH_4 and 50 sccm H_2. Due to the low contrast of bilayers on monolayer graphene using SEM, in this paper, we transferred the graphene films onto SiO_2/Si substrates, and we present here false colored optical images in order to highlight the bilayer regions. The silicon dioxide is represented in white, while the different thicknesses of graphene films are represented in different shades of pink. The bilayer graphene grown on the outside surface of the Cu enclosure can be divided into two stages by comparing the observed growth there to that on a flat substrate.[21] In stage I, bilayers start to form in the middle of the monolayer flakes, while the monolayer, outlined in white, is not yet complete. Both the flat Cu substrate and the enclosure show similar growth behaviors.

However, even after the growth of the monolayer is completed in stage II, the bilayer graphene on the outside of the Cu enclosure continues to grow larger, unlike the bilayers on the flat foils which have stopped growing. Only at much longer times, for example, more than 120 min, does the bilayer on the graphene eventually stop growing (Supporting Information Figure S1). Interestingly, this saturation time coincides very nicely with the growth of monolayer graphene on the inside, as shown in Figure 2. On the inside surface of the Cu enclosure, there is no graphene formation for the first 30 min. It takes much longer for the monolayer on the inside to coalesce into a complete film. For this period of time, the bilayer on the outside surface

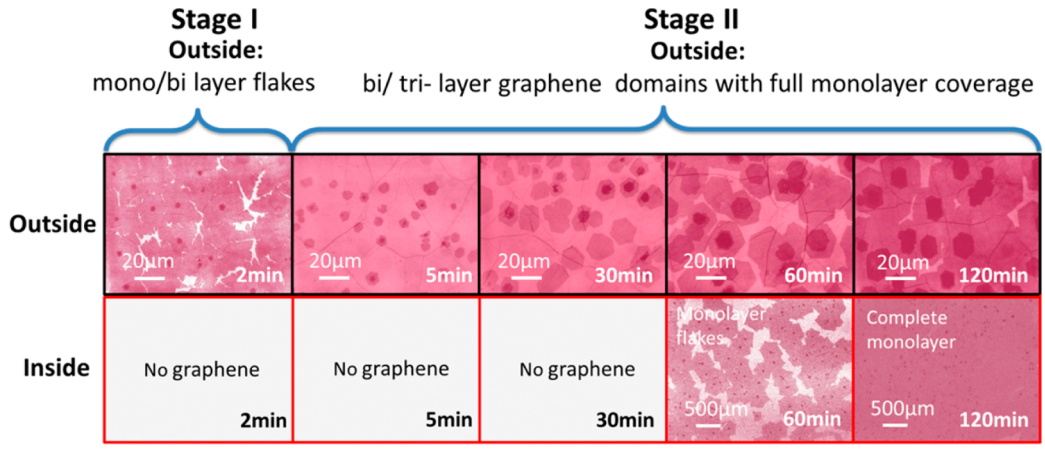

Figure 2. Graphene growth on both sides of the Cu enclosure as a function of time. Here the graphene is transferred onto the SiO_2/Si substrate for better imaging. The different thicknesses of graphene are represented by different shades of pink. On the inside surface, after 60 min, there are some graphene monolayer flakes with a bi/trilayer in the middle. When the growth time is 120 min, the monolayer graphene film growth is completed on the inside, and the bilayer growth on the outside appears to saturate. The graphene growth process is divided into two stages according to the completeness of the monolayer growth on the outside surface of the Cu enclosure.

continues to grow. Once the coverage of monolayer graphene on the inside surface is completed, the bilayer graphene on the outside surfaces also stops growing (Figure S1). Thus, the fraction of exposed Cu on the inside surface appears to affect the growth of bi- and trilayers on the outside Cu surface. This observation strongly suggests that the inside Cu surface plays an important role in supplying additional carbon for the growth of the outside bilayer graphene.

Pathways for Carbon Sources. Since the outside surface of the Cu enclosure is fully passivated within the first few minutes during the growth, the only catalytically active surface capable of providing active carbon is the inside surface of the enclosure. However, if this surface is responsible for the continued bilayer growth, how can the catalytic activity on the inside surface affect the bilayer graphene growth on the outside? To answer this question, we first examined two possible carbon diffusion pathways between the inside and outside surfaces of our enclosures: (1) gaps or holes when forming the enclosure edge and (2) the bulk copper itself. The SEM images at the crimped edges of a typical Cu enclosure (Figure 3a) suggest that carbon can enter the inside of the enclosure through gaps at the edges. This is further confirmed by annealing the Cu enclosure at a higher temperature before growth (see Methods section) to better weld the edges together, which resulted in almost no growth on the inside surface of the enclosure (Figure 3d). Therefore, the graphene monolayer acts as a diffusion barrier, preventing any carbon from the outside from diffusing to the inside.[15] As carbon leaks inside the enclosure, the carbon concentration builds up until a threshold concentration of carbon is reached that is necessary to nucleate graphene.[24] However, if carbon can leak in through these gaps, can carbon species also diffuse out and incorporate with the existing bilayer on the outside? To address this possibility, we crimped a single piece of Cu foil to allow both a flat and an enclosed region to be created side-by-side (Figure 3e). If the active carbon diffuses out through the gaps and goes underneath the monolayer graphene, it should attach to both the

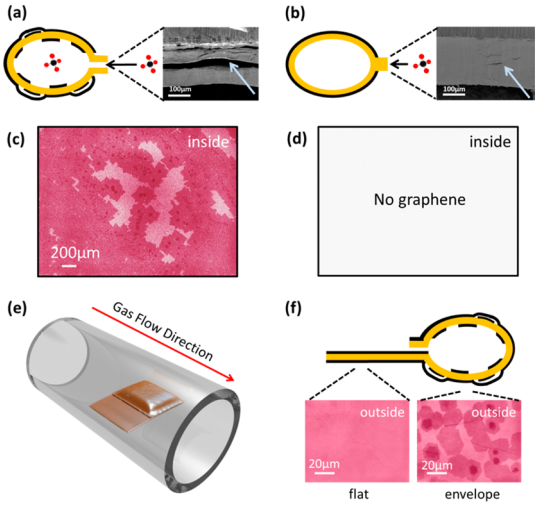

Figure 3. Carbon delivery mechanisms. (a) Schematic of the Cu enclosure with gaps at the crimped edges, and a cross section SEM image on the right confirmed the presence of the gaps. (b) Schematic of the Cu enclosure with better sealed edges, with the corresponding SEM cross section image on the right. (c) Optical images of graphene grown on the inside surface of a Cu enclosure with additional annealing at 1065 °C for 10 min at 420 mTorr. The Cu is first annealed in the shape of an enclosure at 1065 °C. The enclosure is then opened after cooling, and the copper is folded again into a new enclosure as usual (with a gap between the edges). This result indicates that the annealing of the Cu foil does not affect the monolayer graphene growth on the inside surface. (d) No graphene grows on the inside surface when the annealing seals the enclosure at the edges. The growth condition is 1.5 sccm CH_4 and 50 sccm H_2 at 1050 °C for 1 h. (e) Illustration of a sample with both a flat region and an enclosure region where the sample was grown in parallel in the quartz tube. (f) Bilayer regions grow mostly on the enclosure region but not on the flat region.

flat regions and the outside of the enclosure regions, enabling bilayers to grow on both surfaces. On the other hand, if the carbon diffuses through the Cu thickness, there should be a strong preference for bilayers to grow only on the enclosure. After growing for 1 h, we can see that the bilayers are indeed much larger on the enclosure regions as compared to those on the flat regions. As a result, we turn our attention to the second carbon diffusion pathway: diffusion through the bulk of the Cu foil.

If carbon sources actually diffuse through the Cu foil, the growth rate of bilayer graphene films should depend on the thickness of the Cu foil. To test this hypothesis, we utilized an etch mask constructed from Kapton tape in order to protect the outside surface, as well as local regions on the inside surface (Figure 4a). After electrochemical etching (see Methods sections), the Kapton tape was removed and the calculated thickness of the Cu foil was verified by measuring the step heights (~40 μm) using a Dektek profilometer (Figure 4b). After polishing, the roughness of the inside surface decreases.[25] However, the properties of the outside surface of the Cu enclosure were preserved by capping the foil with Kapton tape during the polishing process. We folded the processed Cu foil with the trenched side facing inwards and grew following standard conditions (1.5 sccm CH_4 and 50 sccm H_2 at 1050 °C) for 40 min. The graphene grown on the inside and outside were then transferred to silicon dioxide, as shown in Figure 4c,d, respectively. The positions of the etched regions of the inside of the Cu enclosure are marked in Figure 4c by a dotted line. From Figure 4c, it is interesting to note that the graphene growth on the inside surface has not been perturbed by the etching process and shows a relatively uniform nucleation density. However, on the outside surface (Figure 4d), at low optical magnifications, the transferred graphene from the regions of the thinned Cu foil appear to be optically more absorptive. By examining zoomed-in optical micrographs of these different regions (Figure 4e), we indeed find that the bilayer graphene domain size is much larger on the thinner copper regions as compared to the unetched copper regions. Therefore, the shorter carbon diffusion time in the thinner Cu foil (etched regions) results in a larger amount of carbon at the outside surface available for the growth of bilayer graphene. This is also consistent with previous works that the bilayers grow from underneath the monolayer, as well as other recent work that has shown that carbon can diffuse through Cu thin films to the interface between copper and an insulating substrate to form graphene.[15,20,21,26]

To summarize, the investigations so far suggest that, for the Cu enclosure, the inside environment is *almost* sealed so that methane leaks in very slowly, thereby delaying the Cu passivation on the inside surface. The exposed Cu surface on the inside serves as a catalytic pathway to continuously provide active carbon to the outside surface *via* carbon diffusion through the foil thickness. Potentially, atomic carbon radicals and/or CH_x species could be diffusing through the Cu foil. This asymmetry between the growth rate of graphene on the inside and outside surfaces allows active carbon to diffuse through the Cu foil to grow bilayer graphene.

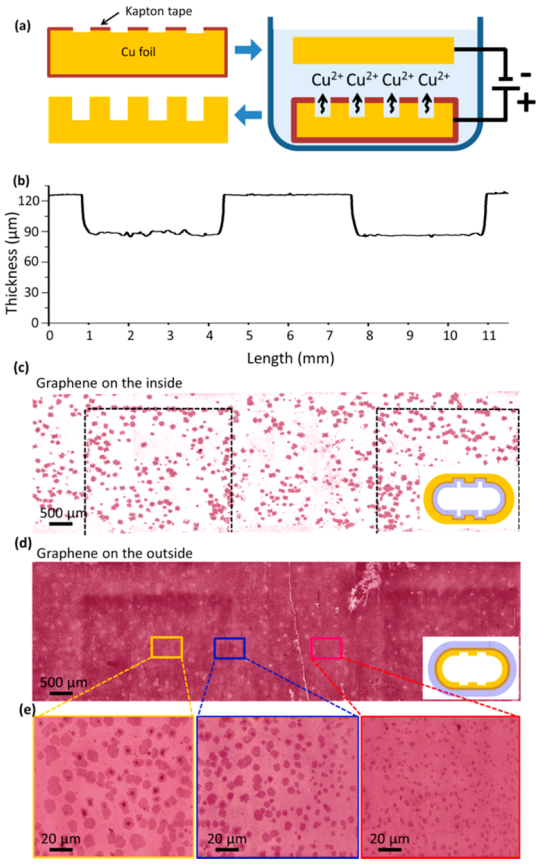

Figure 4. Graphene growth on both surfaces of the Cu foil with the inside surface patterned. (a) Illustration of the patterning process. The sample is covered on one side and patterned on the other side with the Kapton tape. After electrochemically polishing, trenches are formed on only one side. Then the sample was folded with the patterns on the inside, but the outside surface remains the same. (b) Surface profile of the Cu foil surface as measured by surface profilometry (Dektek). (c) Optical images of graphene grown on the inside surfaces of the Cu enclosures. The etched regions are highlighted by the dashed line. The inset in (c) and (d) shows a schematic of the copper enclosure. The highlighted side of the enclosure corresponds to which side of the copper that has been transferred. (d) Comparison of graphene grown on the outside, corresponding to the patterns on the inside. (e) Higher magnification optical images of the graphene grown on the outside surface of the etched regions (orange border), the transition between etched and unetched regions (blue border), and standard copper (red border).

Growth Mechanisms. From the above observations, we propose the following mechanism for the observed two-stage growth of bilayer graphene on the outside surface, as illustrated in Figure 5. During stage I, the processes resemble that of flat copper samples where bilayer graphene growth is independent of the

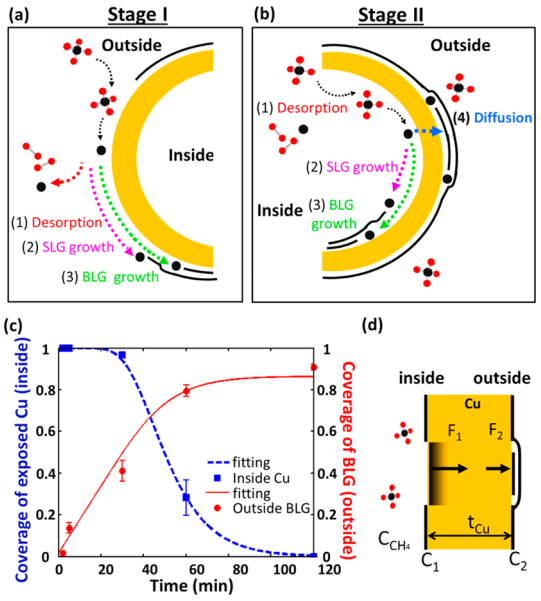

Figure 5. Explanation of the growth mechanisms. (a) Growth mechanism for bilayer graphene on the outside surface in stage I when the monolayer graphene is not complete yet. (b) Growth mechanism for bilayer graphene in stage II after the completion of the monolayer graphene at the outside surface. (c) Fitting of the experimental data to the model for the coverage of the exposed Cu on the inside and the bilayer graphene coverage on the outside *vs* time. (d) Diffusion process for carbon on the inside to go through the copper foil to form a bilayer on the outside underneath the first-grown monolayer graphene.

inside surface. The CH_4 gas adsorbs onto the Cu surface and decomposes to form active carbon species. Most of this active carbon leads to the formation of monolayer graphene while some diffuses underneath the monolayer graphene, resulting in the formation of bilayer flakes. The final size of these bilayers is limited by the rapid growth rate of the monolayer film that serves as a diffusion barrier when grown to completion.[15] Furthermore, the fast completion of the monolayer graphene growth on the outside also prevents carbon diffusion from the outside into the inside. Stage II occurs after the outside monolayer graphene growth is complete. Based on our observations in Figure 2, the inside surface shows no graphene formation for the first 30 min as carbon slowly leaks to the inside through the gaps. Similar to stage I, CH_4 on the inside can decompose and form graphene on the inside surface. However, unlike stage I, due to the slow growth rate of monolayer graphene on the inside, the free surface carbon can either readily diffuse through the Cu foil (to form bilayer graphene on the outside) or form graphene on the inside surface before it is fully covered with monolayer graphene. Thus, the large size of the bilayers on the outside is attributed to the carbon supplied during stage II. As the coverage of monolayer graphene on the inside is almost completed, carbon diffusion through the Cu foil diminishes and the size of the bilayer graphene on the outside saturates.

To better understand the growth mechanism, we model the kinetics of bilayer growth by simultaneously comparing the graphene growth rate on both surfaces. Due to the coupling between the free catalyst area on the inside surface and the bilayer graphene growth on the outside surface, we first analyze the graphene growth on the inside surface, which we assume is independent of the growth of graphene on the outside surface due to the rapid growth rate of the monolayer graphene on the outer surface which acts as a carbon diffusion barrier.[15] It has been reported that the kinetics of monolayer graphene growth on Cu using CH_4 can be represented using a modified Gompertz function.[27] This model applies for graphene growth with the postulation that the graphene grows with a continual carbon input rather than by crystallization from a supersaturated solution.[28] Therefore, we employ this model for the monolayer graphene growth on the inside. The function $p_{in}(t)$ is simplified to represent the coverage of monolayer graphene:

$$p_{in}(t) = \frac{A_{in}(t)}{A_{tot}} = \exp\{-\exp[-R(t - t_0) + 1]\} \quad (1)$$

where $p_{in}(t)$ is the fraction of monolayer graphene coverage on the inside surface of the Cu enclosure, $A_{in}(t)$ is the area of the monolayer (μm^2), and A_{tot} is the total area of the Cu inside surface (μm^2). The value of R (min^{-1}) is determined by the maximum growth rate μ_{max} (μm^2) and the total copper area (A_{tot}); $R = \mu_{max}e/A_{tot}$, where e is Euler's number; t_0 is the time lag (min), which is the time required for the concentration of the active carbon species to achieve a critical supersaturation level for nucleation of graphene to take place.[24] The formation of the active carbon species can occur due to self-pyrolysis of the methane gas as well as by the assisted decomposition of methane from the copper surface.[29,30] Since the direct thermal self-pyrolysis of the methane gas is energetically unfavorable, we focus on the catalytic role of copper, which helps decompose methane more effectively.[31,32] There are a series of steps for the decomposition of CH_4 before the completion of monolayer graphene growth on the inside surface.[30,33] Nevertheless we simplify all the steps into one function, assuming that the governing rate-limiting constant (k_d) is determined by the slowest reaction step with the largest energy barrier E:

$$[CH_4] \xrightarrow{k_d} [C^*], \text{ where } k_d = A\exp\left(-\frac{E}{kT}\right) \quad (2)$$

In eq 2, $[CH_4]$ and $[C^*]$ (#/cm^3) are, respectively, the concentration of methane and active carbon species, while A is a pre-exponential factor, k is the Boltzmann constant, and T is the temperature (K). This equation is valid assuming that there is sufficient methane gas inside the enclosure. The consumption of carbon diffusing through the Cu foil for bilayer growth should be much smaller than the input of carbon into the Cu

enclosure, thereby ensuring that carbon inside the enclosure is never depleted. This assumption is supported by the fact that the monolayer graphene growth on the inside surface keeps increasing over time. Moreover, the concentration of methane is large enough that the monolayer growth can be completed.[34] However, the reaction described above only occurs at regions with an exposed Cu surface. Therefore, to calculate the effective carbon concentration on the inside surface, we need to only consider those regions not covered by graphene $C_1(t)$ (#/cm^3)

$$C_1(t) = (1 - p_{in}(t))C^* \quad (3)$$

The carbon concentration gradient is developed throughout the Cu foil to drive the diffusion process (Figure 4c). $C_1(t)$ (#/cm^3) is the carbon concentration on the inside surface, while $C_2(t)$ (#/cm^3) is that on the outside. We assume that the carbon gets consumed immediately once it arrives at the outer surface, implying $C_2(t)$ is zero. Another assumption is that we only consider diffusion to be one-dimensional (1-D) and there are no carbon sinks within the Cu foil. These assumptions lead to a concentration gradient that is a linear function of distance. Based on our assumptions, the flux of carbon diffusing through the Cu foil ($F_1(t)$ (#/(s·μm^2))) is

$$F_1(t) = D\frac{C_1(t)}{t_{Cu}} \quad (4)$$

Here t_{Cu} is the thickness of the Cu foil and the diffusion coefficient of carbon in the Cu foil is D (μm^2/s). Assuming there is no loss of carbon during the diffusion process, we write $F_1(t) = F_2(t)$, where $F_2(t)$ (#/(s·μm^2)) is the flux of carbon attaching to the bilayer graphene. Combining eqs 1−4, the growth rate for the bilayer is limited by the mass transport of carbon as written in eq 5:

$$\frac{dA_{out}(t)}{dt} = \frac{D}{t_{Cu}} A\exp\left(\frac{E}{kT}\right) A_{tot} C_{CH_4}(1 - p_{in}(t))r \quad (5)$$

where $A_{out}(t)$ is the area of bilayer graphene (μm^2) on the outside surface and r is the areal density of carbon atoms (μm^2/#). (See Supporting Information for more details regarding the derivation of eq 5.)

We plot the coverage of bilayer graphene on the outside surface (red circles) and the percentage of exposed Cu on the inside surface (blue squares) as a function of time in Figure 5d. The fitting curves for the monolayer graphene (dotted blue line) on the inside (eq 1) and for the bilayer graphene (solid red line) on the outside (eq 5) are also shown in Figure 5d. The corresponding curve for bilayer graphene shows good agreement with the experimental data. By extracting the fitting coefficient and by estimating the concentration of methane on the inside surface, we estimate the diffusion coefficient of carbon through the copper to be 3.36 × 10^{-12} m^2/s (see Supporting Information for details), which is an order of magnitude less than the diffusion coefficient of carbon in metals with a higher carbon solubility such as iron (3.6 × 10^{-11} m^2/s at 1050 °C).[35] Therefore, the diffusion coefficient of carbon through the copper microstructure is non-negligible, thereby supporting our assumption that carbon can diffuse through the Cu foil. Other recent work has shown that carbon can diffuse through Cu thin films to the interface between Cu and an insulating substrate to form graphene.[26]

Coverage Dependence on the Thickness of the Cu Foil. To verify our model (eq 5), we also grew bilayer graphene with various thicknesses of Cu foil (t_{Cu}). To utilize the same purity and type of Cu foil throughout the experiment, we purposely varied the thickness of our Cu foil by electrochemically polishing our Cu foil in dilute phosphoric acid (see Methods section). After growth under 1.5 sccm CH_4 and 50 sccm H_2 at 1050 °C for 1 h, the coverage of the bilayers (dotted blue), trilayers (dotted red), and all the carbon content (black) on the outside were plotted as a function of $1/t_{Cu}$ in Figure 6a. The blue line shows that the bilayer coverage saturates around a t_{Cu} of 107 μm; however, eq 5 predicts a linear relationship between the bilayer coverage and $1/t_{Cu}$. To explain for this discrepancy, in most of our previous growth conditions, the inside monolayer graphene coverage has completed before the trilayer coverage has become appreciable; therefore, we have assumed that the integrated carbon content mainly contributes to the bilayer coverage. However, for thinner foils, the carbon delivery rate is much faster than before, such that the trilayer graphene is able to grow before the inside graphene fully passivates the copper surface. In Figure 6c, when the Cu foil was thinned down to 57 μm, the optical image shows that the trilayer graphene becomes almost continuous and even quadlayer graphene starts to appear. However, the percentage of quadlayer coverage is only about 4%.

Our simple model (eq 5) only looks at the total carbon content delivered to the outside surface. Therefore, we plot the total integrated carbon content (black) by summing up the percent coverage of both the trilayer and bilayer graphene. Additionally, based on eq 5, by fitting the coverage *versus* thickness plot, we calculated the diffusion coefficient to be 3.16 × 10^{-12} m^2/s with a goodness of fit (R^2 equals to 0.98). This value is consistent with our previously extracted value 3.36 × 10^{-12} m^2/s, which we obtained through modeling the time-dependent growth of our bilayer graphene on the outside. In Figure 6b, the transmittance of graphene film grown on the Cu enclosure was measured and compared with reference samples of layer-by-layer transferred graphene films. For the reference samples, the transmittance measured at 550 nm was 97.7, 95.35, and 92.96% for 1L, 2L, and 3L of graphene, respectively. Each graphene layer absorbs 2.3 ± 0.1% of the incident light at 550 nm, consistent with other reports from literature.[36] For

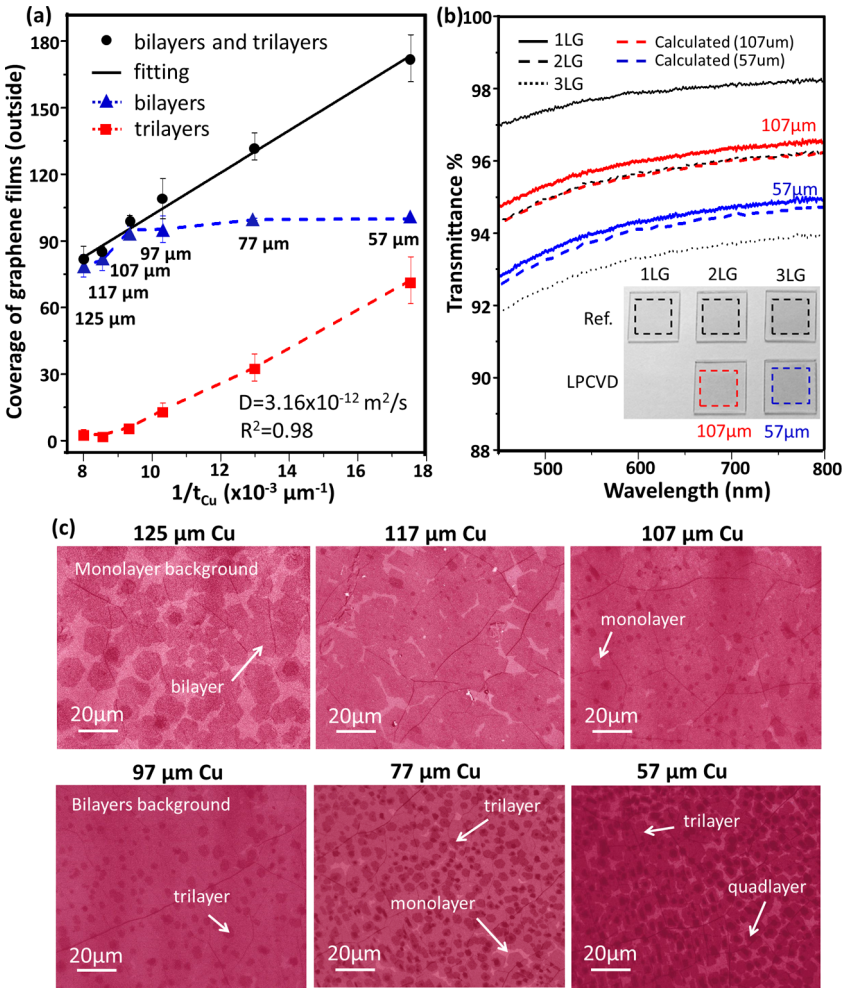

Figure 6. Graphene grown on Cu foil with different thicknesses. (a) Coverage of bilayers (dotted blue), trilayers (dotted red), and the summation of both bilayers and trilayers (dotted black) as a function of thickness of the Cu foil. The linear fitting of the carbon content is shown as a solid black line. (b) Transmittance of the layer-by-layer transferred graphene films (black) and directly grown graphene films on the Cu enclosures with thickness of 107μm (red) and 57 μm (blue), respectively. The inset shows the photograph of the corresponding graphene films on the borosilicate. The layer-by-layer transferred graphene was used as a reference, and the transmittance measured at 550 nm was 97.7, 95.35, and 92.96% with increasing numbers of layers. The transmittance for the LPCVD-grown graphene films at 550 nm was 95.7% (107 μm) and 93.97% (57 μm). (c) Optical images of the graphene films grown on the outside of the Cu enclosure with different thicknesses.

graphene grown on the Cu foil with a thickness of 107 μm, the calculated transmittance given the computed coverage from Figure 6a (1L coverage = 100%, 2L coverage = 94 $\pm$ 2%, 3L coverage = 6 $\pm$ 1.5%) is 95.7%. Additionally, for the graphene films grown on a 57 μm thick Cu foil (1L = 100%, 2L = 100%, 3L = 72 $\pm$ 11%), the total calculated optical transmittance is 93.97%. The small discrepancy (+0.35% for 107 μm and +0.23% for 57 μm) for both films suggests that the film is slightly more transparent than calculated. The small discrepancy in transmittance between the measured and calculated values further confirms the uniformity of bilayer and multilayer films.

CONCLUSIONS

In conclusion, by inspecting the evolution of the two surfaces of the Cu enclosure during the LPCVD synthesis, we have gained a better understanding of the bilayer growth mechanism on the outside surface of the enclosure. It is concluded in this study that the two surfaces are coupled by carbon diffusion through the Cu foil. By identifying the pathways for methane gases and active carbon, we found that carbon diffusing through the Cu foil allows for a continual growth of bilayers from underneath the outside monolayer graphene. On the basis of the monolayer graphene growth on the inside surface and the inter-copper carbon diffusion process, we derived a growth model for the bilayer graphene on the outside which agrees well with the experimental findings. Finally, we verified our model by measuring the thickness dependence of the Cu foil on the delivery rate of carbon. Moreover, utilizing intercatalyst diffusion pathways may serve as a more general method for synthesis of other layer-by-layer hybrid structures, such as graphene on h-BN or isotopic bilayer systems. The improved understanding

of the synthesis of bilayer graphene on copper catalysts will lead to the better control of bilayer graphene growth for future bilayer graphene-based devices and potentially other bilayer nanomaterials.

METHODS

Graphene Growth on Cu Enclosure. The Cu foil (127 μm thick, 99.9%, product no. 13380, lot no. F29X145) was purchased from Alfa Aesar. Before growth, the Cu foil was pretreated by dipping the foil into Ni etchant (nitric acid, Transene Company Inc.) for 30 s, followed by rinsing using DI water. The envelope was made by folding a 1 in. by 2 in. copper strip and crimping the edges using pliers. For electrical polishing, we used phosphoric acid (85%, Macron) mixed with DI water (3:1) as electrolyte. For a typical growth process, the substrate was first heated to 1050 °C under 10 sccm H_2 with a pressure of 350 mTorr for 20 min. Then the substrate was annealed at this temperature under the same condition for 30 min before we started to flow 1.5 sccm CH_4 and 50 sccm H_2. After growth, we turned off the furnace and the substrate was cooled in the same atmosphere. For the Cu enclosures with improved sealing, we crimped the edges as usual and annealed the enclosure at 1065 °C for 10 min at 420 mTorr as an additional step.

Graphene Transfer. We coated the graphene on Cu with a layer of poly(methyl methacrylate) (PMMA, 950 A9, MicroChem, diluted to 4.5% in anisole) at 2500 rpm for 1 min. After coating, we placed the sample in an oven at 80 °C for 10 min. Then the Cu was removed by floating the coated sample on the Cu etchant (CE-100, Transene Company Inc.) for 1 h. Subsequently, we washed the PMMA/graphene and transferred it to a SiO_2/Si substrate. The PMMA was removed by acetone and 3 h thermal annealing at 350 °C under 200 sccm H_2 and 200 sccm Ar.

Characterization. The surface profile was taken by using Dektak Profilometer IIA (Sloan Technology Corp.). SEM images were taken using a Zeiss Supra 40 instrument with an acceleration voltage of 5 keV. The thickness of the Cu foil was also measured by using a digimatic micrometer (Mitutoyo, model MDC-1). Transmittance was measured from the ultraviolet−visible spectrometer (Cary 5000, Varian).

Conflict of Interest: The authors declare no competing financial interest.

Acknowledgment. This work was partially supported by National Science Foundation under award number NSF DMR 0845358 and the Graphene Approaches to Terahertz Electronics (GATE) Multidisciplinary University Research Initiative (MURI) of Massachusetts Institute of Technology (MIT)−Harvard University−Boston University through the Office of Naval Research (ONR), and the Army Research Labs (ARL). M.S.D. acknowledges ONR-MURI-N00014-09-1-1063.

Supporting Information Available: Additional growth results on bilayer graphene and details of the modeling and fitting. This material is available free of charge *via* the Internet at http://pubs.acs.org.

REFERENCES AND NOTES

1. Ohta, T.; Bostwick, A.; Seyller, T.; Horn, K.; Rotenberg, E. Controlling the Electronic Structure of Bilayer Graphene. *Science* **2006**, *313*, 951–954.
2. Oostinga, J. B.; Heersche, H. B.; Liu, X.; Morpurgo, A. F.; Vandersypen, L. M. Gate-Induced Insulating State in Bilayer Graphene Devices. *Nat. Mater.* **2008**, *7*, 151–157.
3. Zhang, Y. B.; Tang, T. T.; Girit, C.; Hao, Z.; Martin, M. C.; Zettl, A.; Crommie, M. F.; Shen, Y. R.; Wang, F. Direct Observation of a Widely Tunable Bandgap in Bilayer Graphene. *Nature* **2009**, *459*, 820–823.
4. Xia, F. N.; Mueller, T.; Lin, Y. M.; Valdes-Garcia, A.; Avouris, P. Ultrafast Graphene Photodetector. *Nat. Nanotechnol.* **2009**, *4*, 839–843.
5. Jablan, M.; Buljan, H.; Soljacic, M. Transverse Electric Plasmons in Bilayer Graphene. *Opt. Express* **2011**, *19*, 11236–11241.
6. Xia, F. N.; Farmer, D. B.; Lin, Y. M.; Avouris, P. Graphene Field-Effect Transistors with High On/Off Current Ratio and Large Transport Band Gap at Room Temperature. *Nano Lett.* **2010**, *10*, 715–718.
7. Reina, A.; Jia, X. T.; Ho, J.; Nezich, D.; Son, H. B.; Bulovic, V.; Dresselhaus, M. S.; Kong, J. Large Area, Few-Layer Graphene Films on Arbitrary Substrates by Chemical Vapor Deposition. *Nano Lett.* **2009**, *9*, 30–35.
8. Kim, K. S.; Zhao, Y.; Jang, H.; Lee, S. Y.; Kim, J. M.; Kim, K. S.; Ahn, J. H.; Kim, P.; Choi, J. Y.; Hong, B. H. Large-Scale Pattern Growth of Graphene Films for Stretchable Transparent Electrodes. *Nature* **2009**, *457*, 706–710.
9. Li, X. S.; Cai, W. W.; An, J. H.; Kim, S.; Nah, J.; Yang, D. X.; Piner, R.; Velamakanni, A.; Jung, I.; Tutuc, E.; *et al.* Large-Area Synthesis of High-Quality and Uniform Graphene Films on Copper Foils. *Science* **2009**, *324*, 1312–1314.
10. Sutter, P. W.; Flege, J. I.; Sutter, E. A. Epitaxial Graphene on Ruthenium. *Nat. Mater.* **2008**, *7*, 406–411.
11. Oshima, C.; Nagashima, A. Ultra-thin Epitaxial Films of Graphite and Hexagonal Boron Nitride on Solid Surfaces. *J. Phys.: Condens. Matter* **1997**, *9*, 1–20.
12. Alstrup, I.; Chorkendorff, I.; Ullmann, S. The Interaction of CH_4 at High Temperature with Clean and Oxygen Precovered Cu(100). *Surf. Sci.* **1992**, *263*, 95–102.
13. Karu, A. E.; Beer, M. Pyrolytic Formation of Highly Crystalline Graphite Films. *J. Appl. Phys.* **1966**, *37*, 2179–2181.
14. Presland, A. E.; Walker, P. L. Growth of Single-Crystal Graphite by Pyrolysis of Acetylene over Metals. *Carbon* **1969**, *7*, 1–4.
15. Nie, S.; Wu, W.; Xing, S. R.; Yu, Q. K.; Bao, J. M.; Pei, S. S.; McCarty, K. F. Growth from Below: Bilayer Graphene on Copper by Chemical Vapor Deposition. *New J. Phys.* **2012**, *14*, 093028.
16. Wu, Y. P.; Chou, H.; Ji, H. X.; Wu, Q. Z.; Chen, S. S.; Jiang, W.; Hao, Y. F.; Kang, J. Y.; Ren, Y. J.; Piner, R. D.; *et al.* Growth Mechanism and Controlled Synthesis of AB-Stacked Bilayer Graphene on Cu−Ni Alloy Foils. *ACS Nano* **2012**, *6*, 7731–7738.
17. Liu, N.; Fu, L.; Dai, B.; Yan, K.; Liu, X.; Zhao, R.; Zhang, Y.; Liu, Z. Universal Segregation Growth Approach to Wafer-Size Graphene from Non-noble Metals. *Nano Lett.* **2011**, *11*, 297–303.
18. Yan, K.; Peng, H. L.; Zhou, Y.; Li, H.; Liu, Z. F. Formation of Bilayer Bernal Graphene: Layer-by-Layer Epitaxy *via* Chemical Vapor Deposition. *Nano Lett.* **2011**, *11*, 1106–1110.
19. Liu, L. X.; Zhou, H. L.; Cheng, R.; Yu, W. J.; Liu, Y.; Chen, Y.; Shaw, J.; Zhong, X.; Huang, Y.; Duan, X. F. High-Yield Chemical Vapor Deposition Growth of High-Quality Large-Area AB-Stacked Bilayer Graphene. *ACS Nano* **2012**, *6*, 8241–8249.
20. Li, Q. Y.; Chou, H.; Zhong, J. H.; Liu, J. Y.; Dolocan, A.; Zhang, J. Y.; Zhou, Y. H.; Ruoff, R. S.; Chen, S. S.; Cai, W. W. Growth of Adlayer Graphene on Cu Studied by Carbon Isotope Labeling. *Nano Lett.* **2013**, *13*, 486–490.
21. Fang, W.; Hsu, A. L.; Caudillo, R.; Song, Y.; Birdwell, A. G.; Zakar, E.; Kalbac, M.; Dubey, M.; Palacios, T.; Dresselhaus, M. S.; *et al.* Rapid Identification of Stacking Orientation in Isotopically Labeled Chemical-Vapor Grown Bilayer Graphene by Raman Spectroscopy. *Nano Lett.* **2013**, *13*, 1541–1548.
22. Li, X. S.; Cai, W. W.; Colombo, L.; Ruoff, R. S. Evolution of Graphene Growth on Ni and Cu by Carbon Isotope Labeling. *Nano Lett.* **2009**, *9*, 4268–4272.
23. Li, X. S.; Magnuson, C. W.; Venugopal, A.; Tromp, R. M.; Hannon, J. B.; Vogel, E. M.; Colombo, L.; Ruoff, R. S. Large-Area Graphene Single Crystals Grown by Low-Pressure Chemical Vapor Deposition of Methane on Copper. *J. Am. Chem. Soc.* **2011**, *133*, 2816–2819.

24. Kim, H.; Mattevi, C.; Calvo, M. R.; Oberg, J. C.; Artiglia, L.; Agnoli, S.; Hirjibehedin, C. F.; Chhowalla, M.; Saiz, E. Activation Energy Paths for Graphene Nucleation and Growth on Cu. *ACS Nano* **2012**, *6*, 3614–3623.
25. Han, G. H.; Gunes, F.; Bae, J. J.; Kim, E. S.; Chae, S. J.; Shin, H. J.; Choi, J. Y.; Pribat, D.; Lee, Y. H. Influence of Copper Morphology in Forming Nucleation Seeds for Graphene Growth. *Nano Lett.* **2011**, *11*, 4144–4148.
26. Su, C. Y.; Lu, A. Y.; Wu, C. Y.; Li, Y. T.; Liu, K. K.; Zhang, W. J.; Lin, S. Y.; Juang, Z. Y.; Zhong, Y. L.; Chen, F. R.; *et al.* Direct Formation of Wafer Scale Graphene Thin Layers on Insulating Substrates by Chemical Vapor Deposition. *Nano Lett.* **2011**, *11*, 3612–3616.
27. Winsor, C. P. The Gompertz Curve as a Growth Curve. *Proc. Natl. Acad. Sci. U.S.A.* **1932**, *18*, 1–8.
28. Celebi, K.; Cole, M. T.; Choi, J. W.; Wyczisk, F.; Legagneux, P.; Rupesinghe, N.; Robertson, J.; Teo, K. B. K.; Park, H. G. Evolutionary Kinetics of Graphene Formation on Copper. *Nano Lett.* **2013**, *13*, 967–974.
29. Olsvik, O.; Rokstad, O. A.; Holmen, A. Pyrolysis of Methane in the Presence of Hydrogen. *Chem. Eng. Technol.* **1995**, *18*, 349–358.
30. An, W.; Zeng, X. C.; Turner, C. H. First-Principles Study of Methane Dehydrogenation on a Bimetallic Cu/Ni(111) Surface. *J. Chem. Phys.* **2009**, *131*, 174702.
31. Zhang, W. H.; Wu, P.; Li, Z. Y.; Yang, J. L. First-Principles Thermodynamics of Graphene Growth on Cu Surfaces. *J. Phys. Chem. C* **2011**, *115*, 17782–17787.
32. Lacava, A. I.; Bernardo, C. A.; Trimm, D. L. Studies of Deactivation of Metals by Carbon Deposition. *Carbon* **1982**, *20*, 219–223.
33. Losurdo, M.; Giangregorio, M. M.; Capezzuto, P.; Bruno, G. Graphene CVD Growth on Copper and Nickel: Role of Hydrogen in Kinetics and Structure. *Phys. Chem. Chem. Phys.* **2011**, *13*, 20836–20843.
34. Li, X. S.; Magnuson, C. W.; Venugopal, A.; An, J. H.; Suk, J. W.; Han, B. Y.; Borysiak, M.; Cai, W. W.; Velamakanni, A.; Zhu, Y. W.; *et al.* Graphene Films with Large Domain Size by a Two-Step Chemical Vapor Deposition Process. *Nano Lett.* **2010**, *10*, 4328–4334.
35. Scourse, F. P.; Smithells, C. J. *Metals Reference Book*; Butterworth & Co. Publishers Ltd.: London, 1967.
36. Nair, R. R.; Blake, P.; Grigorenko, A. N.; Novoselov, K. S.; Booth, T. J.; Stauber, T.; Peres, N. M. R.; Geim, A. K. Fine Structure Constant Defines Visual Transparency of Graphene. *Science* **2008**, *320*, 1308–1308.